trast between the ocean water and the rock, g is the gravity acceleration, and λ is the wavelength of the relief. By use of Eq. 1 and the spreading velocity ($v = s/t$) of 2 cm/year, we can then solve for the viscosity:

$$\eta = \rho g \lambda s_e / 4\pi v \qquad (2)$$

where s_e is the distance in which the relief falls to $1/e$ of its original value. Equation 2 then expresses the unknown value for the viscosity in terms of quantities that are known or that can be determined from the profiles of the Mid-Atlantic Ridge.

The amplitudes of the relief of the published Mid-Atlantic Ridge profiles (*6*, *8*) were plotted versus their distance from the Central Rift Valley, and an exponential function was fitted by the least-squares method.

The result of the analysis of one of the profiles (*6*) is shown in Fig. 1. The viscosity thus derived is between 1.5 and 3.9×10^{22} poises, and the most probable value is 2.1×10^{22} poises.

A similar analysis of the other profile (*8*) indicates an apparent change in the viscosity at some point in the past. From the Central Rift Valley to a point about 160 km to the west, we obtain a viscosity value of 4.6×10^{22} poises by least-squares analysis; beyond 160 km we obtain 8.2×10^{22} poises. This apparent change in the viscosity may be real, but it is also possible that the viscosity is the same but that the spreading velocity was greater in the past. Since there is evidence (*9*) that the spreading rate has decreased along other portions of the Mid-Atlantic Ridge, it seems more likely that the change in the spreading velocity is the cause of the discrepancy.

A geographical difference in spreading rates may partly explain the discrepancy in the derived value for the viscosity from each of the profiles. The profile graphed in Fig. 1 crosses the Mid-Atlantic Ridge at about 25°N, and the other profile crosses at 28°40′S. As observed by Heirtzler *et al.* (*10*), the spreading rate at the first location is between 1.25 and 1.4 cm/year, and the second location has a spreading rate of 1.95 cm/year. This difference in spreading rate would tend to move the value derived from the first profile closer to the value derived from the second, until they would be within the error of the least-squares analysis.

We have used a very simple model despite the vast differences between the horizontal dimensions of Fennoscandia and the relief of the Atlantic bottom. These results are therefore surprisingly consistent and are in good agreement with the value derived by Haskell (*3*).

CHRIS H. CRAMER
University of Puget Sound,
Tacoma, Washington 98416

References and Notes

1. F. R. Eirich, Ed., *Rheology, Theory and Applications* (Academic Press, New York, 1962).
2. A. E. Scheidegger, *Principles of Geodynamics* (Springer-Verlag, Berlin, 1958), pp. 64–115, 265–271.
3. N. A. Haskell, *Physics* **6**, 265 (1935); **7**, 56 (1936); *Amer. J. Sci.* **233**, 22 (1937).
4. M. D. Crittenden, *J. Geophys. Res.* **68**, 5517 (1963).
5. For a review of current hypotheses, see R. K. McConnell, *ibid.*, **73**, 7087 (1968); D. L. Turcotte and E. R. Oxburgh, *ibid.* **74**, 1458 (1969), who also examined older theories. For a mathematical treatment of the subject, see Z. F. Daneš, *Icarus* **9**, 1 (1968); *ibid.*, p. 8.
6. B. C. Heezen, M. Tharp, M. Ewing, *The Floors of the Oceans, The North Atlantic* (Geological Society of America, Special Paper 65, New York, 1959), vol. 1, p. 91.
7. H. Lamb, *Hydrodynamics* (Dover, New York, 1945), pp. 625–628.
8. M. Ewing, X. Le Pichon, J. Ewing, *J. Geophys. Res.* **71**, 1620 (1966).
9. J. D. Phillips, *Science* **157**, 920 (1967).
10. J. R. Heirtzler, G. O. Dickson, E. M. Herron, W. C. Pitmann, X. Le Pichon, *J. Geophys. Res.* **73**, 2119 (1968).

26 September 1969

Transverse Wave Instability in a Solid Explosive

Abstract. *By the use of a metal indentation technique, microscopic transverse or side-running shock waves can be detected in composition C-4, an explosive consisting largely of cyclonite (RDX) with organic plasticizers. The minimum wave spacing observed is approximately 0.05 millimeters, with a lateral velocity of about 6.5 millimeters per microsecond. The instability was demonstrated in cylindrically divergent detonation waves.*

There is considerable experimental evidence that the assumption of stability of flow behind the plane detonation front is valid only under special conditions. For gas detonations, it has been established that turbulence, transverse oscillations, and multiheaded spinning detonations occur under various conditions, even far from where boundary layer effects would be important (*1*, *2*).

Similar phenomena are also manifested in liquid explosives, such as nitromethane (*3*), and in transparent liquid explosives (*4*). It is the purpose of this report to present experimental evidence for the existence of microscopic transverse wave instability in a solid explosive material.

The particular formulation used in the preliminary experiments was composition C-4, consisting of 91 percent RDX (also called cyclonite, whose formula is $C_3H_6N_6O_6$), 2 percent polyisobutylene, 2 percent motor oil, and 5 percent di-(2-ethylhexyl) sebacate. The RDX particle size is less than 0.04 mm.

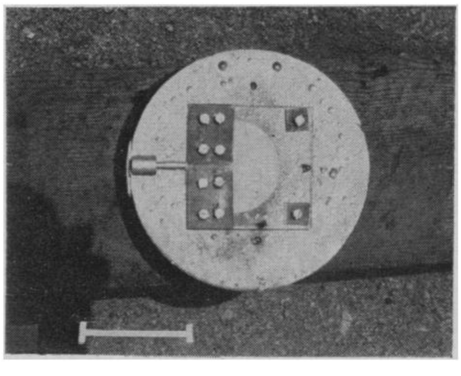

Fig. 1. Top view of the experimental arrangement. The scale line is 10 cm.

The indentation technique was employed to record the fluctuations in pressure along the detonation front (*5*, *6*). In this method a polished metal surface is placed in intimate contact with the explosive. On recovery, after the detonation wave has passed over the plate, the small permanent plastic deformations of the metal surface can be photographed with grazing-incidence illumination. The technique might be considered a high-pressure analog of the smoked-foil method employed to record similar oscillatory phenomena in gaseous detonations, but at much lower pressures (*2*).

It seemed most likely that a microscopic transverse wave instability, if it existed, would be manifested under cylindrical divergence (a geometry in which the occurrence of steady detonation is open to question), and also under a condition of failure, where the detonation wave is no longer self-supporting at its free-running, stable, high-order, Chapman-Jouguet velocity. To produce these conditions, the explosive layer was initiated from the center and the detonation front propagated into a layer of decreasing thickness.

Figure 1 shows the experimental arrangement. For recovery purposes a

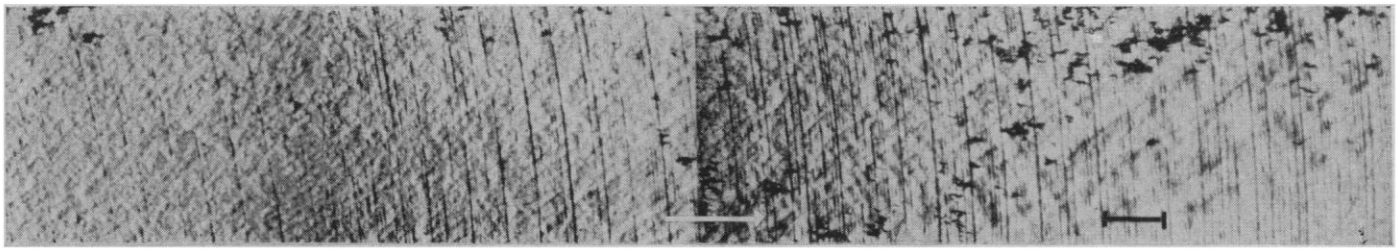

Fig. 2. Surface of stainless steel disk showing opposed logarithmic spirals engraved by intersection of transverse waves and the detonation front (which, as the arrow indicates, propagated from left to right). The vertical arcs are machined marks; the black spots, local carbon deposits. The scale line is 1 mm.

fairly massive experiment is desirable. A disk of stainless steel, 1.3 cm thick, is polished and cut along the diameter. One of these halves is then cast into a cylinder of lead. Because of the somewhat plastic consistency of composition C-4, the explosive could be compressed by a Lucite cover plate into thin hemicircular wedge disks having a density of 1.65 g/cm^3. (The crystal density of RDX is 1.82 g/cm^3.) Center initiation was effected by an explosive train leading out to a detonator. The explosive thickness varies from 3 mm at the upper side of the semicircle to 0.5 mm on the lower side.

Figure 2 is a mosaic of three photomicrographs of a sector of the recovered steel surface, near the diameter of the hemicircle and at a radius of 4 cm. The thickness of the explosive layer at the left end of the record was approximately 1.1 mm; at the right end, 0.9 mm.

The pattern of opposed logarithmic spirals shows the loci of the intersections of side-running transverse shock waves and the detonation front, the engravement being due to a localized increase in pressure at the intersection. The vertical arc scratches are due to tooling marks which were deliberately left, in the polishing process, to indicate the relative depth of engravement of the spiral traces. The dark spots on the surface are due to local deposition of carbon from the detonation products.

Several qualitative features of this record should be noted. First, the minimum spacing between the waves, along the detonation front, is quite small, being about 0.05 mm in the left part of the record, increasing, as the detonation wave begins to fail, to approximately a millimeter at the right end. Also, the pressure at the intersection of transverse wave and the detonation front increases toward the right end of the record, if one judges by the increase of deflection of the arc scratches.

Figure 3 is an area of the center part of Fig. 2, at higher magnification and with grazing-incidence illumination, to demonstrate the varying depth of engravement and the general features of the surface. This record also shows more clearly the waves having minimum spacing.

One must be careful in the attribution of surface effects caused by exposure of metal samples to high-explosive detonation products. In certain geometries, similar patterns can also be caused by metal strains. The traces shown in Figs. 2 and 3, however, are not due to such phenomena, for the direction of the explosively produced stress is normal to that which could conceivably produce such patterns and, furthermore, the surface features do not have the character of edges of slip planes but are, rather, true surface engravements. Also, the increase of the wave spacing and engravement depth as the detonation pressure decreases is strong evidence against such an interpretation. The presence of Helmholtz two-layer instability waves at the explosive-metal interface can also leave permanent surface waves on the metal, but these are characterized by a train of irregular waves nearly parallel to the direction of the detonation front.

I have also observed the transverse waves under conditions quite different from those in the experiments described above. They also occur in composition C-4 that has been preshocked (*5*), which renders the explosive insensitive by removing initiation sites. The transverse wave instability appears in such material under conditions of high overdrive (behind detonation wave Mach stems or in cylindrically convergent detonation waves). The minimum wave spacing is about 0.2 mm in these cases.

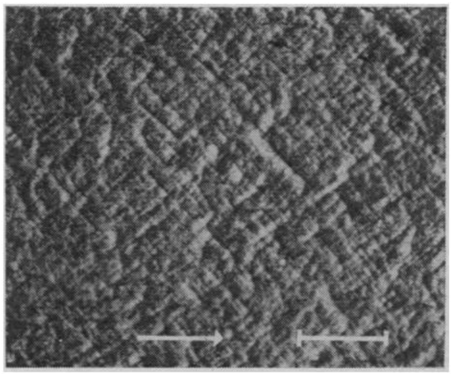

Fig. 3. At higher magnification, the fine structure of the engraved traces appears. The minimum spacing between the transverse wave intersections, along the detonation front (which, as indicated by the arrow, propagated from left to right), is approximately 0.05 mm. The scale line is 1 mm.

The length of the reaction zone in composition C-4 has been estimated, from values of this parameter in explosives having similar constituents, to be about 0.15 mm. The minimum spacing of the transverse waves, as measured in the microphotograph shown in Fig. 3, is approximately 0.05 mm and, since the spacing of transverse waves in gas detonations is usually not smaller than the length of the reaction zone, a shorter reaction zone may be indicated for this explosive. It is also possible, of course, that the RDX particle size may influence the observed minimum wave spacing.

The observed increase of pressure and of the spacing between the transverse waves, which is noted in Fig. 2, as the detonation begins to fail, is a characteristic of this instability in a gas detonation (*7*).

The appearance of the transverse waves demonstrates that, under the conditions of the experiments, the flow in the reaction zone is not one-dimensional, and stable, but rather oscillatory. The oscillation frequency of this reaction zone flow can be determined by dividing the minimum spacing of the transverse waves (0.05 mm) into their lateral speed (6.5 mm/μsec), giving a value of approximately 130 Mhz.

B. B. Dunne
Science Applications, Inc.,
P.O. Box 2351, La Jolla, California

References

1. A. K. Oppenheim, N. Manson, H. G. Wagner, *Amer. Inst. Aeronaut. Astronaut. J.* **1**, 2243 (1963); D. R. White, *Phys. Fluids* **4**, 465 (1961); R. E. Duff, *ibid.*, p. 1427.
2. Y. H. Denisov and Y. K. Troshin, *Dokl. Akad. Nauk SSSR* **125**, 110 (1959) [transl. *Phys. Chem. Sect.* **125**, 217 (1960)]; *Zh. Tekh. Fiz.* **30**, 450 (1960); K. I. Shtshelkin, *Dokl. Akad. Nauk SSSR* **47**, 501 (1945).
3. A. W. Campbell, T. E. Holland, M. E. Malin, T. P. Cotter, *Nature* **178**, 38 (1956); H. Dean Mallory, *J. Appl. Phys.* **38**, No. 13, 5302 (1967).
4. H. Dean Mallory and R. A. Plauson, *Nature* **199**, 18 (1963).
5. B. B. Dunne, *Phys. Fluids* **4**, 918 (1961).
6. ———, *ibid.*, p. 1565.
7. R. I. Soloukhin, *Shock Waves and Detonations in Gases* (Mono, Baltimore, 1966), p. 138.

6 October 1969; revised 10 December 1969 ■

Electron Population Parameters from Least-Squares Refinement of X-ray Diffraction Data

Abstract. *A least-squares refinement of x-ray diffraction data has been developed in which the parameters are the populations of atomic orbital products describing the molecular electron density distribution. The procedure is applied to α-oxalic acid dihydrate and cyanuric acid. Complementary structural information obtained by neutron diffraction has been used. In the absence of complementary information, the method allows simultaneous determination of structural and charge-density parameters. There is an indication of a migration of charge from the* p_π *to the* p_σ *orbitals in both molecules.*

A number of recent studies have shown that information on the electron distribution in molecules can be obtained from diffraction data (*1–5*). The redistribution of electrons upon the formation of a molecule has been illustrated through Fourier difference maps, obtained either through a combination of x-ray and neutron diffraction data (*2, 3*), or by use of parameters from high-order x-ray refinements (*4, 5*).

Such Fourier maps are illustrative but do not provide quantitative information for direct comparison with theoretical calculations. An alternative procedure, outlined here, is the determination by least-squares refinement of x-ray diffraction data of parameters describing the electron density.

If the molecular orbitals ψ_i are mutually orthogonal linear combinations of atomic orbitals φ_μ, with coefficients $C_{i\mu}$, the one-electron density function ρ is described by a summation of orbital products $\varphi_\mu\varphi_\nu$, each multiplied by an appropriate population coefficient $P_{\mu\nu}$:

$$\psi_i = \sum_\mu C_{i\mu} \varphi_\mu \tag{1}$$

$$\rho = 2 \sum_\mu \sum_\nu \sum_i^{\text{occ}} C_{i\mu} C_{i\nu} \varphi_\mu \varphi_\nu \equiv \sum_\mu \sum_\nu P_{\mu\nu} \varphi_\mu \varphi_\nu \tag{2}$$

The evaluation of the x-ray scattering of the density described by the orbital products $\varphi_\mu\varphi_\nu$ is facilitated considerably when the atomic orbitals are expressed as linear combinations of Gaussian type orbitals. The appropriate expressions and constants have been given by Stewart (*6*).

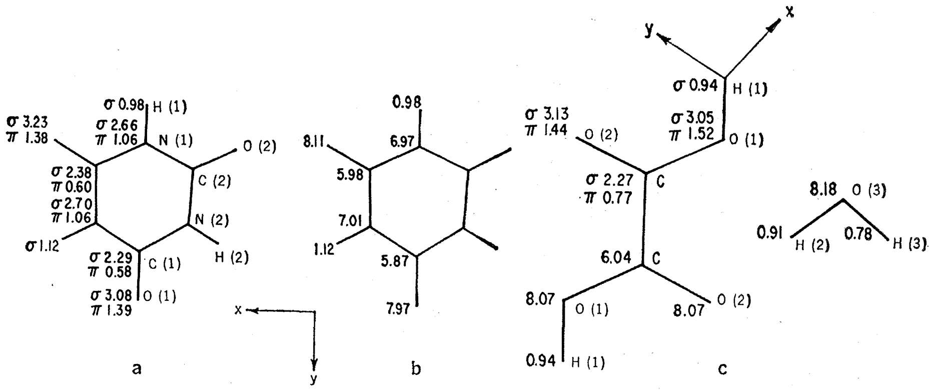

Fig. 1. Experimental charge distributions in cyanuric acid (a and b), and in α-oxalic acid dihydrate (c) obtained with the Hartree-Fock basis set. Figure 1a and the upper half of the oxalic acid molecule in Fig. 1c show the division into p_σ *and* p_π populations, whereas the total charge distribution is given in Fig. 1b and the remaining part of Fig. 1c. The two halves of the oxalic acid molecule and the two halves of the cyanuric acid molecule are related by crystallographic symmetry elements. The $2s^2$ populations of the C, N, and O atoms are set at 1.0, 1.25, and 1.50 electrons, respectively.

The x-ray observations give information on the electron density time-averaged over the vibrations of the molecule in the crystal. In the present treatment we allow for thermal motion by assuming that each one-center orbital product experiences the same motion as the nucleus on which it is centered, whereas the two-center orbital products are assumed to vibrate with a mean-square amplitude which is the average of the amplitudes of the two centers.

We have tested two different models. In the first, a one-center model, all cross products between orbitals on different atoms are neglected. In the second model, a limited multicenter model, cross products between adjacent covalently bonded atoms in the molecule are included. In the calculations reported here a minimum Hartree-Fock (HF) basis set of $1s$, $2s$, $2p_x$, $2p_y$, and $2p_z$ orbitals for carbon, nitrogen, and oxygen atoms and $1s$ orbitals for hydrogen atoms is used. The method is by no means limited, however, to a Hartree-Fock basis set. Indeed, similar calculations with Slater-type orbitals have been completed.

The $1s$ electrons of the C, N, and O atoms are assumed to be unperturbed by bonding, thus eliminating $1s^2$ population coefficients as parameters in the least-squares refinement. Short-range migrations of charge near the nucleus are not observable with this technique, because of the limited resolution of the x-ray diffraction data.

Early experience indicated a large correlation between the $2s^2$ population and a spherical sum of the $p_x{}^2$, $p_y{}^2$, and $p_z{}^2$ orbital products, resulting from the almost equal radial dependences of the time-averaged $2s$ and $2p$ orbitals (*6*). The $2s^2$ population was therefore fixed at an arbitrary value in subsequent calculations. A full description of the asphericity of the valence electrons was obtained by variation of the population of the $p_x{}^2$, $p_y{}^2$, and $p_z{}^2$ orbital products. Hence nine one-center population parameters are included for each heavy atom in a general crystallographic position; they are the coefficients $P_{\mu\nu}$ listed in Tables 1 and 2. Symmetry requirements reduce the number of parameters for atoms in special positions.

Using positional and thermal parameters obtained by neutron diffraction, we applied the one-center model to the x-ray diffraction data on α-oxalic acid dihydrate (*3*) and cyanuric acid (*4*).